

This is a self-archived version of the original publication.

The self-archived version is a publisher's pdf of the original publication.

To cite this please use the original publication:

Sivula, A., Maula, H., Koskela, H., Hongisto, V. 2023. Air flow patterns and draught risk caused by the collision of supply jets. Proc. 18th Healthy Buildings Europe Conference. p. 553-558. 11th - 14th Jun 2023, Aachen, Germany

All material supplied via Turku UAS self-archived publications collection in Theseus repository is protected by copyright laws.

More information on self-archiving contact julkaisutiedonkeruu@turkuamk.fi

Air flow patterns and draught risk caused by the collision of supply jets

Arttu Sivula, Henna Maula, Hannu Koskela, Valtteri Hongisto

Built Environment Research Group, Turku University of Applied Sciences, Turku, Finland, arttu.sivula@turkuamk.fi

Abstract. In office buildings, complaints about the thermal environment are often related to temperature or sensation of draught. Some of the challenges in finding solutions when designing comfortable workspaces are related to the complexities of the air flow patterns. In this paper, the effect of the collision of supply air jets on the airflow pattern and the draught risk in a single office room were analysed. The experimental situation created for the study is a typical draught situation in offices, where high heat loads has led into increased cooling to sustain the room temperature at a desired level. This paper is part of a larger study on thermal comfort and the draught situation was created for the purposes of human experiment. The focus of this paper is in analysing the airflow pattern under the created draught conditions. The airflow pattern was visualized with smoke and quantified with physical measurements and the draught risk was calculated. The downfall jet from the colliding supply jets caused local maximum air speeds directly above the workstation and the calculated draught risk was above the recommended values. The results show the strong effect of convective airflows on air distribution.

Keywords. Thermal comfort, draught risk, airflow pattern, air speed

1. Introduction

Thermal comfort is defined as the condition of mind that expresses satisfaction with the thermal environment and is used to describe how pleasant or unpleasant the thermal conditions are (ASHRAE 55:2020). Thermal comfort is affected by air temperature, radiant temperature from the surfaces, air movement, relative humidity, and personal factors, such as, body composition, age, clothing, and activity level (ISO 7730:2005).

The most common complaints regarding the thermal environment in offices are related to air temperature and feeling of draught (IFMA, 2009). Draught is defined as the unwanted local cooling caused by the movement of air (ASHRAE 55:2020). A typical problem in office environments occurs when increased space efficiency increases the need for cooling. The increased local air movement can unintentionally have a negative impact on the thermal comfort of the occupants and eventually cause discomfort. At a high temperature, the movement of the air can be perceived as pleasant, while in cooler conditions, humans are more sensitive to draught and air movement can have a negative effect on comfort (Toftum, 2004).

HVAC systems aim to maintain comfortable thermal conditions indoors as thermal comfort is important

for wellbeing and productivity of the occupants (Seppänen et al., 2006). International and national standards have been set to give recommendations for design and target values for, e.g., room temperature and air velocity with respect to good indoor environment quality (e.g., ISO 7730:2005, EN 16798-1:2019, ASHRAE 55:2020) The indoor environment can be classified based on the criteria set in these standards. The criteria reflect the acceptable quality described usually from higher to lower (e.g., category A to C in ISO 7730:2005) and can be used for the evaluation and design of the thermal environment. The correct operation of HVAC systems is essential in providing and maintaining acceptable levels of occupant thermal comfort and requires good design. Managing thermal comfort for different occupants is challenging. For one, the management of airflows in the room space is difficult. The air flow patterns in the room are complex and are influenced by the supply air device and the amount strength and location of the heat loads in the space. High internal loads can be particularly challenging when trying to keep thermal conditions within acceptable levels.

It is therefore important to increase the understanding on the effects of different HVAC solutions and heat loads on the air flow patterns in the occupied zone, especially in typical situations where the room air temperature is within the recommended

values and the thermal comfort of the occupants can be assumed to be close to neutral.

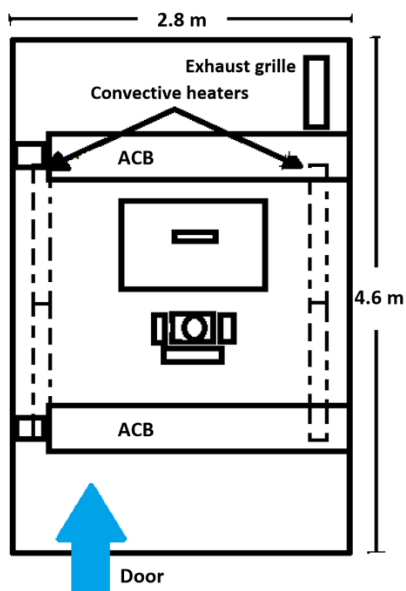
In this paper, the effects of the collision of supply air jets on the airflow pattern and the associated draught risk (DR) in a single office room were analysed. The experimental condition was a draught situation typical to office environments. It was created in laboratory for the purposes of human experiment as part of a larger study focusing on thermal comfort. The perceived thermal comfort of the human experiment will be discussed in another publication by Maula et al. (2023).

2. Methods

In this experiment, a draught situation typical to office environments was created, in which high heat loads have led to increased cooling to sustain the temperature in the room at a desired level. The study was carried out in the psychophysics laboratory of Turku University of Applied Sciences in a 13 m² room (h=2.8 m) furnished as a single person office room. The experimental room layout is illustrated in Figure 1.

Figure 1

Experimental Room Layout: Workstation located between Active Chilled Beams (ACBs) and convective heaters



The high air speeds causing draught at the workstation were created by using a high internal heat load (111 W/m²) and correspondingly high cooling power. The internal heat loads are summarized in Table 1. Cooling and the fresh air were supplied into the room with two Active Chilled Beams (ACBs). ACBs induce room air through a cooling coil and mix it with the primary air. The mixture is

supplied into the room as supply air. The distance between the ACBs was 2.0 m. The workstation was placed in an area between the two ACBs as this area has potential for increased DR. The primary air flow rate was 70 L/s (5.4 L/s*m²). The cooling water inlet temperature was 14 °C and the outlet temperature was 16 °C. The supply air temperature at the measuring point at the supply slot was 19.4 °C. The average temperature measured at the workstation was 22.8 °C.

Table 1

Internal heat loads in the room.

Heat load component		W	W/m ²
Occupant	Heated dummy	70	5.5
Equipment	Display	27	2
Lighting	2xLED modules	58	4.5
Other heat loads	Convective heaters	1290	99
Total		1445	111

The air flow pattern was illustrated with smoke visualizations. The smoke was produced with a smoke machine (Stairville SF-1000 MKII) and released into the supply air duct. The smoke movement was recorded with a camera. During the recording, the walls of the room were covered with a black fabric, and additional lights were used to distinguish the smoke more clearly from the background.

For quantitative evaluation of the created test situation, air speed, temperature, and turbulence intensity were measured in the area between the ACBs, and the draught risk was calculated based on the ISO 7730 standard as Eq. (1)

$$DR = (34 - t_a)(V_0 - 0.05)^{0.62} (0.37 \cdot V_0 \cdot Tu + 3.14) \quad (1)$$

where: t_a [°C] is the air temperature, V_0 [m/s] is the mean air speed (≥ 0.05 m/s) and Tu [%] is the turbulence intensity. The measurements were done with hot sphere anemometers (Dantec Dynamics A/S, Denmark) with 3-minute averaging time. The anemometers were attached to a height-adjustable bar (length 2.0 m) with 0.1 m spacing, allowing the measurements to be displayed with a 0.1 x 0.1 m mesh. The horizontal plane flow field measurements were made from heights of 0.1 m (ankle), 1.5 m (0.1 m above the top of the heated dummy), 1.8 m (upper limit of the occupied zone) and 2.3 m (level of the

underside of the ACBs). The measurements on vertical plane were made from the heights between 0.1–2.3 m in the middle of the area where the seated person would sit in the human experiment. Measurements were made both with and without the heated dummy. The selected heights were influenced by the limitations imposed by the measuring equipment.

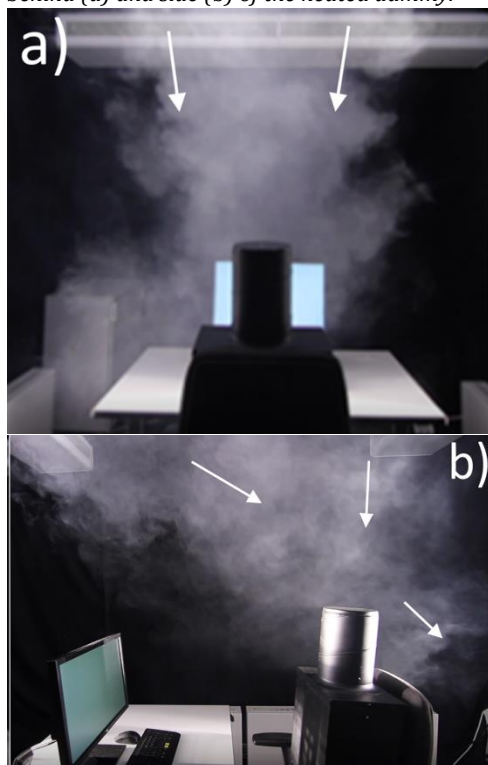
3. Results

3.1 Airflow visualization

The smoke visualizations were used to illustrate and qualitatively evaluate the airflow patterns. Still images of the recorded smoke flow are shown in Figures 2 and 3a. Figure 2a show that the downfall jet formed from the collision of the supply jets from the two opposing ACBs descends towards the workstation and begins to spread towards the long sides of the room. Figure 2b illustrates that the downfall jet descends to the head and face area from the ACB in front of the heated dummy and to the back of the neck from the ACB located behind the dummy.

Figure 2

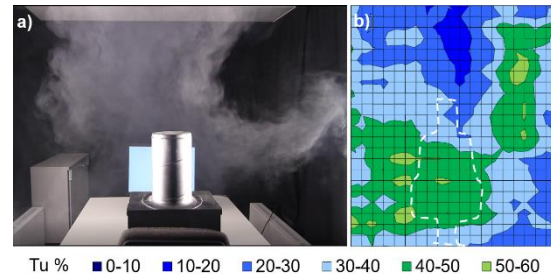
Supply air flow pattern visualized with smoke from behind (a) and side (b) of the heated dummy.



The convection currents generated by the convective heaters turn the falling smoke upwards on the right side of the room and cause large turbulent flow structures. The area of higher turbulence on the right side of the room is verified in the vertical turbulence intensity distribution (Fig 3b).

Figure 3

Smoke visualization of the airflow pattern of the downfall jet affected by the convective heaters (a) and vertical turbulence intensity distribution from heights of 0.1–2.3 m (b).

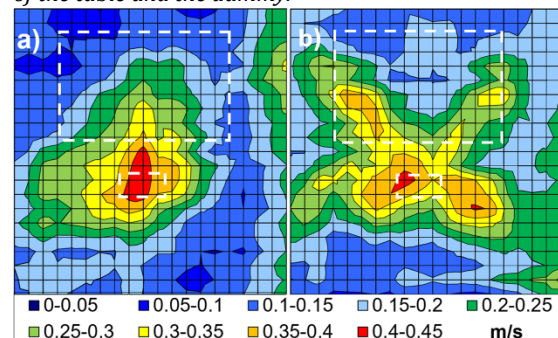


3.2 Air speed

Both vertical and horizontal planes were measured with hot sphere anemometers from different heights to quantify the air distribution. Some of the air speed distributions from the horizontal measurements are shown in Figure 4. The highest air speeds were above the workstation with the local maximums directly above the chair. The area of higher air speed is narrower on top of the table than above the chair. The air speeds reduced with increasing distance from the centre of the chair. The maximum air speeds were measured at the height of 2.3 m (0.5 m/s) just below the ACBs. The maximum measured air speeds above the top of the heated dummy ($h=1.5$ m) were higher than 0.4 m/s.

Figure 4

Horizontal Air speed distribution from heights of 1.5 m (a) and 2.3 m (b). The dotted lines depict the positions of the table and the dummy.

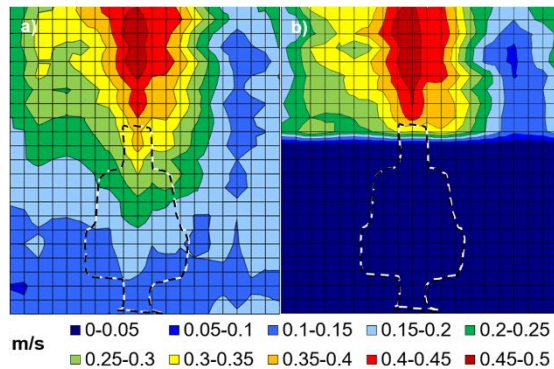


The vertical air speed distributions are shown in Figure 5. The air speeds of the downfall jet decrease along with the decreasing distance to the floor. At the neck height (1.1 m) the air speeds were approx. 0.25 m/s (max. 0.3 m/s) and at the pelvic height (0.6 m) the air speed was 0.15 m/s. The lowest air speeds were measured at the height of 0.1 m (<0.13 m/s) that is at an ankle level of a seated person. The air speed distribution above the heated dummy is very similar

without the heated dummy (Fig 5a) and with the dummy (Fig 5b).

Figure 5

Vertical Air speed distributions without the heated dummy from heights between 0.1-2.3 m (a) and with the heated dummy (b). The dotted lines depict the position of the dummy.

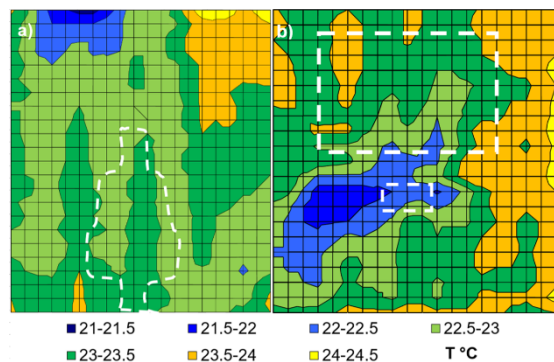


3.3 Air temperature

Some of the air temperature measurement results are shown in Figure 6. The temperature was 0.2 °C higher at ankle height than at head height (1.1 m). The temperature was higher than the surrounding environment above the convective heaters in the upper part of the room as shown on the right side of both Fig 6a and b. The horizontal temperature distribution at the height of 2.3 m (Fig 6b) show that temperature is cooler than the rest of the environment in the area behind and left of the position of the heated dummy.

Figure 6

Vertical temperature distribution from heights of 0.1-2.3 m (a) and horizontal temperature distribution from height of 2.3 m (b). The dotted lines depict the positions of the table and the dummy.



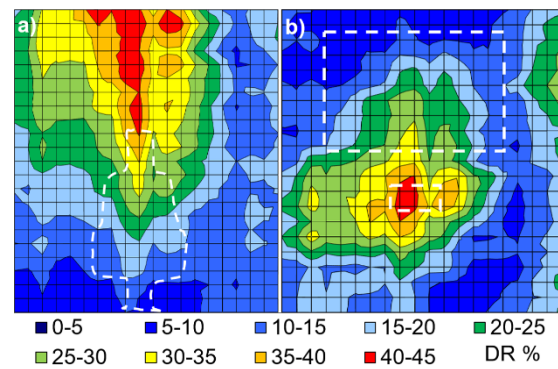
3.4 Draught risk

The distributions of the DR correlated with the air speed distributions. Figure 7 show that the local maxima of DR were directly above the seated person.

The vertical measurement level (Figure 7a) shows that the DR is lower closer to the floor. The DR at neck height (1.1 m) of the sitting person was about 25 % (max. value 32 %) and at the pelvic height approx. 15% (max. 20%). The draught risk at the workstation was lowest at ankle height (10 %). Above the head height and up to the upper limit of the occupied zone (1.8 m), the DR was in the range of 30–35% (highest value 46 %).

Figure 7

Vertical DR distribution from heights of 0.1–2.3 m (a) and horizontal DR distribution from height of 1.5 m (b). The dotted lines depict the positions of the table and the dummy.



4. Discussion

4.1 Airflow pattern

Based on the smoke visualizations and the physical measurements, the airflow pattern was dominated by the HVAC solution and the location of the heat loads. The supply jets from the two opposing ACBs collided closer to the door side wall and the resulting downfall jet caused local maximum air speeds directly above the seated person. This kind of flow pattern was set up intentionally to create draught conditions for human experiment. The air speeds of the downfall jet were highest in the area directly above the seated person and reduce vertically as the downfall jet descended towards the floor (Figures 4,5).

The formation of the collision jet closer to the door side wall highlights the complexities of the room airflow patterns. The shape of the downfall jet is affected by the interaction with the heat sources placed on each side of the room. Fig 4a and 5 show that the air speeds are lower on the right side of the table. This is due to upward convective flow of warmer air from the convective heaters on the right side of the room opposing and deflecting the downward flow of the collision jet towards the workstation. The cooler downfall jet is also induced to the right at various points due to the air pressure difference caused by the rising convection current as seen above the table level in Fig 3a. The phenomenon is visible also from the

shape of the temperature distribution on the right of the heated dummy in Fig 6a, as the area of cooler air is induced up towards the top of the convective heater on the right.

The effect of the table and its location on the airflow pattern was not studied extensively here. It is noteworthy that the workstation is not placed exactly in the middle of the room, as the table is 0.2 m closer to the right-hand wall and convective heaters to allow easier passage to the back of the room, and a lot closer to the back wall. Also, each of the presented distribution figures shown are measured 0.3 m closer to the wall on the right. This position gives a better understanding of the airflow pattern close to a wall as the measurement bar was too short (2.0 m) to allow the measurement of the whole room width simultaneously.

The shape and formation of the downfall jet closer to the door side wall could possibly be affected by temperature differences between the two opposing supply jets. Fig 6b show that the temperature is cooler in the area behind and left of the workstation. Unfortunately, the temperature of the supply air from the ACBs was only measured from one supply slot (of one ACB) and from one measurement point instead of measuring from multiple locations around both ACBs. Therefore, assumptions are based on Fig 6 and cooling coil layout of the ACBs used. The cooling coil water pipe connections are located on either side of the front end next to primary air connection. In the studied room, both ACBs were installed so that the primary air connection is on the left side wall of the room. The chilled water inlet pipe has been installed on the left side and the chilled water outlet on the right side of front end in both ACBs. Therefore, the strongest cooling capacity would be immediately after the water inlet point as the temperature of the chilled water rises (as the water absorbs the heat from the induction air) as it circulates through the cooling coil. Thus, the supply air from the left side of the ACB would be slightly cooler than the supply air from the right side. This means that from the two supply jets directed towards the workstation the air from the supply jet (of the ACB) closer to the door wall would be cooler which coincided with temperature distribution in Fig 6b. The cooler temperature could cause the supply air to descend earlier than the warmer air due to buoyancy effect, leading to the formation of a collision jet closer to the door side ACB. The lack of accurate temperature data from different points of the ACBs mean that further investigation would be needed before drawing solid conclusions.

The locations of the workstation, heat sources and the exhaust grille and the air currents produced by the ACBs may all affect the symmetry and destabilize the airflow field. Strong convection currents can form large air circulations in room affecting the symmetry

of the airflow patterns and making it difficult to predict the airflow patterns in the room space.

The presence of the heated dummy appears to have little effect on the shape, or the air speeds, of the downfall jet. It seems that the downfall jet is effective in displacing the plume of the heated dummy indicating that the downfall jet can be assumed to remain the same even when a real person is working at the workstation.

4.2 Draught risk

The objective of creating high air movement at the workstation that people perceive unpleasant was successful. Based on the results, the distribution of DR correlated well with the air speed distributions, i.e., in the areas of the highest air speeds, the DR was also the highest. This is logical as the temperature across the measured area was close to 23 °C and the DR model depends on the air speed, the air temperature, and the turbulence intensity (ISO 7730:2005).

In the created draught situation, the DR at neck height of 1.1 m and above is above the target values set in category C defined by ISO 7730:2005. The area below the neck height of 1.1 m could be considered to belong to either category C or B but the draught model may overestimate the predicted DR below the neck height (EN 16798-1:2019). The air speeds at pelvic height and below meet the values recommended for occupants engaged in near sedentary physical activity (<0.2 m/s at <23°C) by ASHRAE 55:2020, but at neck height the target values were exceeded.

Neck and head region are the most sensitive to draught due to not being covered with clothing (ASHRAE 55:2020). Based on the results, the DR % achieved at neck level in the created situation is above the recommended values. No vertical temperature stratification between head and ankle level was formed that could cause other kind of thermal discomfort. Furthermore, the plume of the thermal dummy did not appear to have a significant effect on the shape or air speeds of the downfall jet and thus the air flow pattern is expected to remain the same with the presence of human beings. Thus, the objective to create draught situation in the workstation has been successful. However, the perception of draught is highly individual and the effect of the created situation on perceived thermal comfort has been studied with test subjects and the results are presented in the article by Maula et al. (2023).

5. Conclusion

The air flow pattern and draught risk in the created experimental situation were assessed in a single person office room setup with high heat load. The setup was created in laboratory for draught perception studies with human test subjects. The

results indicate that the predicted proportion of dissatisfied persons in the created experimental situation is above the recommended values and thus, the creation of draught situation was successful.

The results presented in this article describe the air flow pattern scenario forming in the space when, due to high thermal loads (in this case $111/\text{Wm}^2$), the cooling capacity has been increased to sustain the temperature in the room at a desired level. The results also emphasise the importance of good design in the placement of workstations and in creating and maintaining of good indoor climate.

6. Acknowledgements

This study was carried out within the project “Motti - indoor environment and wellbeing in offices” (2020-2024), which is implemented by Turku University of Applied Sciences. Its main funder is Business Finland Ltd (2682/31/2019). The other funders are Audico Systems Ltd, Framery Ltd, Halton Ltd, Martela Ltd, Pietiko Ltd, Rockwool Finland Ltd, University Properties of Finland Ltd, Turku University of Applied Sciences Ltd, and Ministry of the Environment of Finland. This study is part of IEA EBC Annex 87 Energy and Indoor Environmental Quality Performance of Personalized Environmental Control Systems.

7. References

ANSI/ASHRAE (2020) Standard 55:2020, Thermal Environmental Conditions for Human Occupancy. ASHRAE, Atlanta.

EN ISO 7730 (2005). Ergonomics of the thermal environment. Analytical determination and interpretation of thermal comfort using calculation of the PMV and PPD indices and local thermal comfort criteria. International Organization for Standardization, Geneva.

IFMA (2009). Temperature Wars: Savings vs. Comfort, International Facility Management Association (IFMA), Tech. Rep.

Toftum, J. (2004). Air movement – good or bad?. *Indoor Air*, 14: 40-45. doi.org/10.1111/j.1600-0668.2004.00271.x

Seppänen O., Fisk W.J., Lei QH. (2006). Effect of temperature on task performance in office environment. Lawrence Berkeley National Laboratory, 2006, *LNBL report 60946*. <https://escholarship.org/uc/item/45g4n3rv>

EN 16798-1 (2019). Energy performance of buildings. Ventilation for buildings. Part 1: Indoor environmental input parameters for design and assessment of energy performance of buildings addressing indoor air quality, thermal environment, lighting and acoustics. Module M1-6

Maula, H., Sivula, A., Radun, J., Tervahartiala, I-K., Hongisto, V. (2023). The influence of colliding supply jets on predicted and perceived thermal comfort. *In proceedings of the 18th Healthy Buildings conference, 11-14 June 2023, Aachen, Germany.*